Simple 2 × 2 MIMO 60-GHz Optical/Wireless System With Extending Fiber Transmission Distance

Hou-Tzu Huang, Chun-Ting Lin, Ya-Tang Chiang, Chia-Chien Wei, and Chun-Hung Ho

***Abstract*—This paper presents a simple 2 × 2 multiple-input multiple-output (MIMO) 60-GHz radio-over-fiber system. Due to the proposed specific frequency arrangement of driving signals, each optical transmitter requires only a single-drive Mach-Zehnder modulator with 3-dB bandwidth of less than 35 GHz. This arrangement of frequencies can increase the tolerance of optical signals to dispersion-induced RF fading, thereby extending fiber transmission distance. Unfortunately, this scheme leads to signal-to-signal beating interference (SSBI), which can deteriorate system performance. Thus, we employed a 2 × 2 MIMO scheme to enhance data capacity by combining two data streams and two corresponding SSBIs prior to signal demodulation. We also developed a novel iterative equalization technique to mitigate SSBI in the MIMO system. The proposed system achieved a maximum capacity of 55.9-Gb/s in the transmission of 7-GHz orthogonal frequency division multiplexing signals over 12-km fiber and 3.5-m air transmission using a bit-loading algorithm.**

***Index Terms*—Multiple-input multiple-output (MIMO), optical fiber communication, signal processing algorithms, wireless communication.**

I. Introduction

CONSIDERABLE research has gone into the development of multi-gigabit-per-second access networks to meet the demands of integrated broadband services, such as VoIP, HDTV, and multimedia services. Achieving maximum capacity without increasing system costs is the primary challenge in this field. The enormous growth of wireless applications has moved wireless local access networks to the forefront of cellular networks. Increasing the frequency of wireless signals is an efficient means to achieve required data rates and in 2001 the FCC allocated 7-GHz (57–64 GHz) of bandwidth in the unlicensed spectrum [1].

Unfortunately, higher frequencies increase free-space fading [2]. Radio-over-fiber (RoF) systems have shown considerable promise as a network architecture capable of extending the coverage of mm-wave signals [3]–[10]. RoF systems take advantage of fiber transmission to overcome propagation loss and expensive equipment can be centralized to reduce system costs. Nevertheless, the distance of fiber transmission in conventional optical double-sideband (DSB) RoF systems is limited by dispersion-induced RF-fading [11]. We previously proposed a number of 60-GHz OFDM RoF systems to overcome this issue [12], [13], thereby extending transmission distance from 500 m to 4 km [12]. In this study, we organized the frequencies of optical RF tone and optical signals to decrease dispersion-induced RF-fading. These efforts resulted in signal-to-signal beating interference (SSBI) in a single-input single-output RoF system [14]. Nonetheless, the implementation of an iterative SSBI mitigation algorithm enabled the extension of fiber transmission distance beyond 10 km with minimal fading.

This paper proposed the combining of two transmission data streams and two corresponding SSBIs using multiple-input multiple-output (MIMO) technology to expand transmission capacity. Training symbols were used to characterize the information of MIMO channels in order to separate the two data streams using their own SSBI. The use of iterative SSBI mitigation for the separation of data streams enables the recovery of the two data streams without affecting the MIMO channel or SSBI. We also employed a bit-loading algorithm, which made it possible to attain a capacity of 50 Gb/s using 7-GHz OFDM signal over 3.5-m wireless and 6-km fiber transmission. Even after replacing the 6-km fiber with a 12-km fiber, a capacity of 40 Gb/s was maintained.

A number of previous researchers have investigated 2 × 2 MIMO schemes [15]–[18]. The systems in [15] and [16] used coherent detection, which requires lasers with a particularly narrow bandwidth laser in the remote antenna unit (RAU). Due to the direction (vertical/horizontal) of the antenna arrangements in [15] and [17], the wireless signals were nearly independent and the signal bandwidth exceeded 7 GHz, resulting in relatively low spectral efficiency. The single carrier, and signal in [18], requires an additional filter to eliminate undesired signals, which increases costs.

This article is organized as follows. Section II introduces the concept behind the proposed 2 × 2 MIMO 60-GHz RoF system and iterative SSBI mitigation algorithm. Section III details the operations of the proposed MIMO system. Section IV discusses the experimental results according to the design criteria outlined in Section II. Section V lays out the main contributions of this article and presents our conclusions.

II. Concept of Proposed System

Fig. 1 presents a conceptual depiction of the modulation scheme used in the proposed 60-GHz OFDM RoF system, based on a single-drive Mach-Zehnder modulator (SD-MZM) [12]. The SD-MZM is biased at the null point and operated in the

Manuscript received January 15, 2014; revised February 26, 2014; accepted March 23, 2014. Date of publication April 21, 2014; date of current version September 1, 2014.

H.-T. Huang, C.-T. Lin, and C.-H. Ho are with the Institute of Photonic System, National Chiao-Tung University, Tainan 711, Taiwan (e-mail: whang.kurt@gmail.com; jinting@mail.nctu.edu.tw; cunhonho@gmail.com).

Y.-T. Chiang and C.-C. Wei are with the Department of Photonics, National Sun Yat-sen University, Kaohsiung 804, Taiwan (e-mail: peterc1215@gmail.com; ccwei@mail.nsysu.edu.tw).

Color versions of one or more of the figures in this paper are available online at http://ieeexplore.ieee.org.

Digital Object Identifier 10.1109/JLT.2014.2317695

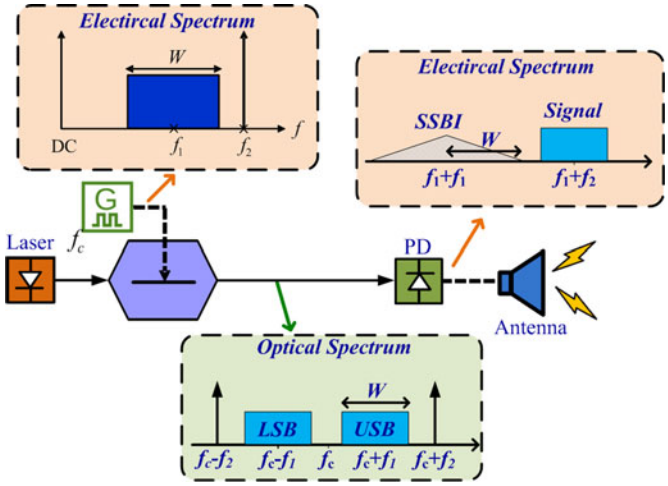

Fig. 1. Simple 60-GHz 2 × 2 MIMO-OFDM RoF system with utilizing SD-MZM.

linear E/O region to achieve an optical DSB signal with carrier suppression. Disregarding the nonlinearity of the SD-MZM, the optical spectrum is simply an up-converted version of the electrical spectrum of the driving signal, comprising an OFDM signal with bandwidth of W at the central frequency of f_1 and a sinusoidal carrier at the frequency of f_2. Assuming that the complex amplitudes of the carriers and the nth subcarrier are respectively C and D_n in the upper side band, then they will be C^* and D_n^* in the lower side band, where $*$ denotes the complex conjugate. Considering only the effects of dispersion, the photo current generated by the nth OFDM subcarrier in the desired 60-GHz frequency band can be expressed as follows:

$$i_{\mathrm{OFDM}}(n) = 4R_{PD}\Re\{C \cdot D_n e^{j2\pi(f_1+f_2+n\Delta f)t}\} \times \cos(2\pi^2\beta_2 L[(f_1+n\Delta f)^2 - f_2^2]), n = \pm 1, \pm 2, \ldots, \pm\frac{N}{2} \quad (1)$$

where R_{PD} is the responsivity of the photo-detector, Δf is the subcarrier spacing, $-W/2 \le n\Delta f \le W/2$ is the relative frequency of the subcarrier with respect to the center frequency of f_1, N is the number of subcarriers, L is the fiber distance, and β_2 is the fiber group velocity dispersion parameter. The exponential term in (1) implies that the beating term is generated at $f_1 + f_2 + n\Delta f$, which falls within the desired 57 to 64-GHz band, i.e. $f_1 + f_2 = 60.5$ GHz and $W = 7$ GHz, and, the cosine term denotes the dispersion-induced fading of RF power. In addition to the desired RF signal, the beating terms between the optical OFDM signals in both side-bands represent the undesired SSBI. As shown in Fig. 1, the spectra of SSBI falls in the range between $2f_1 - W$ and $2f_1 + W$. To avoid in-band SSBI, f_1 and f_2 must be selected, such that $2f_1 + W \le f_1 + f_2 - W$ or $f_2 - f_1 \ge 3W/2$. Therefore, according to Eq. (1), the equality holds in the case of the least fading without in-band SSBI; i.e, $f_1 = 25$ GHz and $f_2 = 35.5$ GHz [12]. Nonetheless, power fading can be minimized by selecting

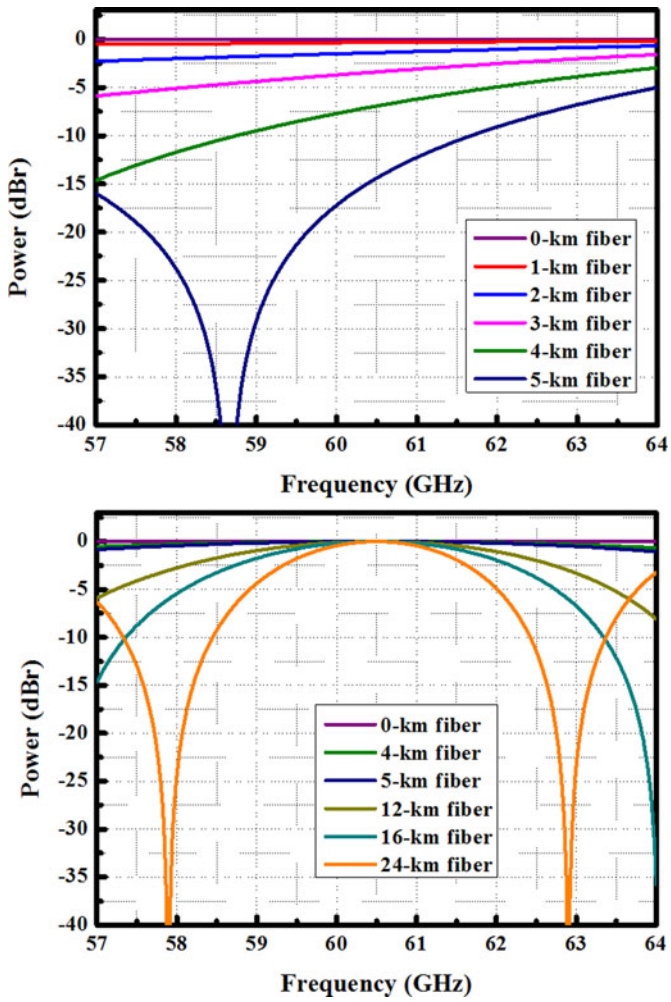

Fig. 2. Simulation results of RF fading at 60-GHz band versus different fiber lengths. (a) $f_1 = 25$ GHz, $f_2 = 35.5$ GHz. (b) $f_1 = f_2 = 30.25$ GHz.

$f_1 = f_2 = 30.25$ GHz, such that the fading term changes to $\cos(n\theta_n)$, where $\theta_n = 2\pi^2\beta_2 L\Delta f \times (2f_1 + n\Delta f)$. Fig. 2(a) and (b) present the RF power fading in cases where $f_1 = 25$ GHz and $f_2 = 35.5$ GHz, and $f_1 = f_2 = 30.25$ GHz, respectively. Simulation results represent power relative to the case of 0-km fiber transmission. β_2 of -21.66 ps^2/km was used to consider single-mode fiber transmission. The signal in the first case is subject to a power penalty of more than 40 dB following fiber transmission over a distance of 5-km. In contrast, the signal in the second case suffers from fading of less than 10 dB even after 12-km fiber transmission. Nonetheless, the price paid to minimize fading is the presence of in-band SSBI, which can be deterministically calculated and removed at the receiver [19].

This study employed a 2 × 2 MIMO scheme to increase the capacity of 60-GHz wireless signals over an RoF system. We adopted the frequency arrangement of $f_1 = f_2 = 30.25$ GHz to minimize RF fading. The unavoidable in-band SSBI and the desired 60-GHz OFDM signals are combined in the wireless channel, as shown in Fig. 3. In the 2 × 2 MIMO system, the

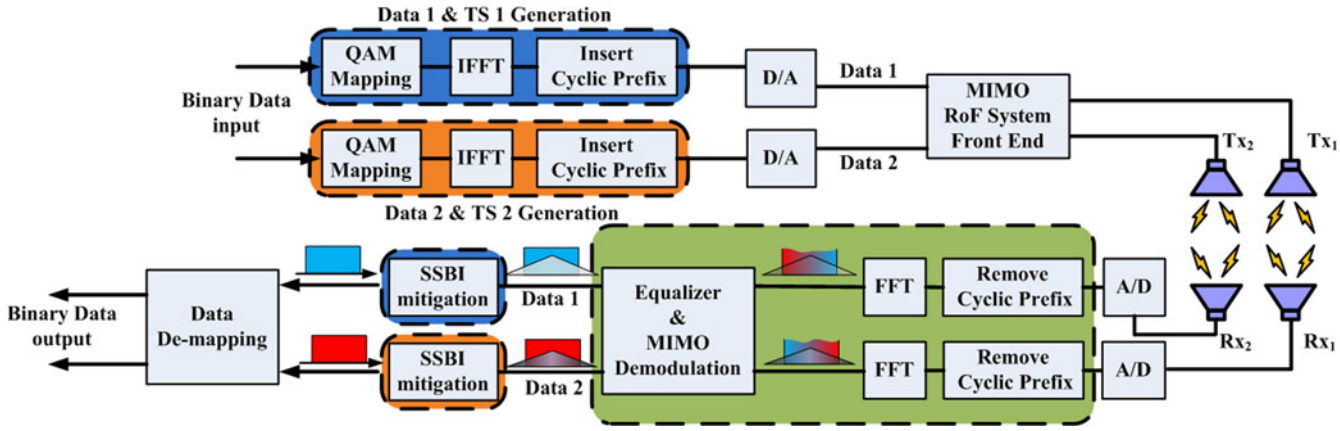

Fig. 3. The proposed 2 × 2 MIMO-OFDM DSP process incorporating SSBI mitigation algorithm.

model of the wireless channel can be expressed as follows:

$$\begin{bmatrix} Y_{1,n} \\ Y_{2,n} \end{bmatrix} = \begin{bmatrix} H_{11,n} & H_{12,n} \\ H_{21,n} & H_{22,n} \end{bmatrix} \times \begin{bmatrix} X_{1,n} + S_{1,n} \\ X_{2,n} + S_{2,n} \end{bmatrix} + \begin{bmatrix} W_{1,n} \\ W_{2,n} \end{bmatrix} \tag{2}$$

where $X_{i,n} = D_n \cos(n\theta_n)$ represents the transmitted nth subcarrier from the ith transmitter antenna (Tx_i), and $Y_{j,n}$ represents the received nth subcarrier at the jth receiver antenna (Rx_j). $S_{i,n}$ stands for the SSBI of the nth subcarrier at the transmitter antenna of Tx_i, $W_{i,n}$ denotes the additive noise of the nth subcarrier, and $H_{ji,n}$ is the channel coefficient from Tx_i to Rx_j. Utilizing the discrete convolution, $S_{i,n}$ can be written as [21],

$$S_{i,n} = \frac{1}{C}\left[\frac{1}{2}D^2_{i,\frac{n}{2}} + \sum_{m=\left\lfloor \frac{n}{2}+1 \right\rfloor}^{\frac{N}{2}} D_{i,m} D_{i,n-m} \cos\left((2m-n)\theta_n\right)\right] \tag{3}$$

where $\lfloor x \rfloor$ denotes the largest integer less than or equal to x, and $D_{i,k} = 0$ as $k \notin \{\pm 1, \pm 2, \ldots, \pm N/2\}$. Moreover, separating the two transmitted signals at the receiver requires a MIMO channel matrix, which can be estimated by sending training symbols. To prevent the interference of channel estimation by the SSBI, the even subcarriers of the training symbols are denoted as null, as shown in Fig. 4 [20]. Among the training symbols, the SSBI exists only in null subcarriers because the SSBI is generated from even subcarriers, in which the frequency spacing is the multiple $2\Delta f$. Thus, least-square estimation of the odd-subcarrier MIMO channel is performed as follows:

$$\cos(n\theta_n)\begin{bmatrix} \tilde{H}_{11,n} & \tilde{H}_{12,n} \\ \tilde{H}_{21,n} & \tilde{H}_{22,n} \end{bmatrix} = \begin{bmatrix} \mathbf{Y}^{\mathrm{TS}}_{1,n} \\ \mathbf{Y}^{\mathrm{TS}}_{2,n} \end{bmatrix} \times \begin{bmatrix} \mathbf{D}^{\mathrm{TS}}_{1,n} \\ \mathbf{D}^{\mathrm{TS}}_{2,n} \end{bmatrix}^{-1}, \quad n \in \text{odd} \tag{4a}$$

where $\mathbf{D}^{\mathrm{TS}}_{1,n}$ and $\mathbf{Y}^{\mathrm{TS}}_{1,n}$ are the row vectors, of which the elements are the $D_{i,n}, Y_{j,n}$ of the training symbols, respectively. Nonetheless, even subcarriers are not sent, such that their MIMO channel can be estimated via interpolation,

$$\tilde{H}_{ji,n} = \frac{1}{2}\left(\tilde{H}_{ji,n-1} + \tilde{H}_{ji,n+1}\right), \quad n \in \text{even}. \tag{4b}$$

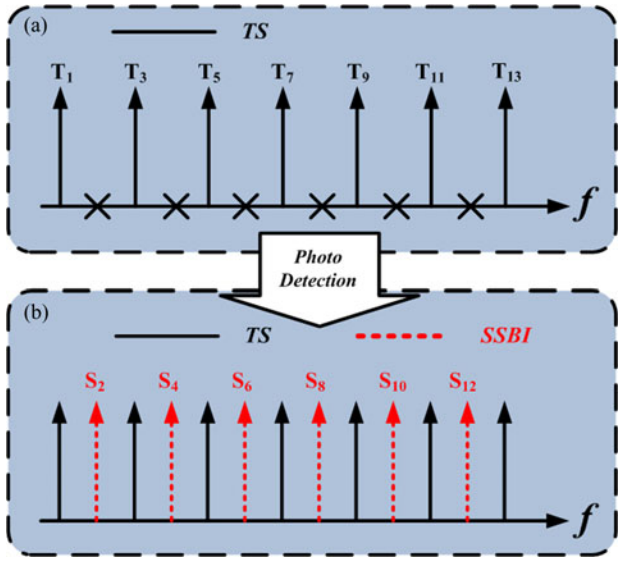

Fig. 4. Simple 60-GHz 2 × 2 MIMO-OFDM RoF system with utilizing SD-MZM.

Using such an approach, the channel matrices of all subcarriers can be reliably estimated without SSBI. As shown in Fig. 3, following the removal of the cyclic prefix (CP) and fast Fourier transform, the MIMO wireless channel coefficient can be determined using the training symbols with Eq. (4). The subsequent application of the zero forcing algorithm [19] enables the estimation of SSBI-interfered data as $\tilde{D}_{1,n}$,

$$\begin{aligned} \begin{bmatrix} \tilde{D}_{1,n} \\ \tilde{D}_{2,n} \end{bmatrix} &= \sec(n\theta_n)\begin{bmatrix} \tilde{H}_{11,n} & \tilde{H}_{12,n} \\ \tilde{H}_{21,n} & \tilde{H}_{22,n} \end{bmatrix}^{-1} \times \begin{bmatrix} Y_{1,n} \\ Y_{2,n} \end{bmatrix} \\ &= \begin{bmatrix} D_{1,n} + S_{1,n}\sec(n\theta_n) \\ D_{2,n} + S_{2,n}\sec(n\theta_n) \end{bmatrix} \\ &\quad + \sec(n\theta_n)\begin{bmatrix} \tilde{H}_{11,n} & \tilde{H}_{12,n} \\ \tilde{H}_{21,n} & \tilde{H}_{22,n} \end{bmatrix}^{-1} \begin{bmatrix} W_{1,n} \\ W_{2,n} \end{bmatrix}. \end{aligned} \tag{5}$$

Equation (5) indicates that the two SSBI would be decoupled by zero forcing, such that the SSBI mitigation algorithm can be applied individually without the need to consider MIMO [14].

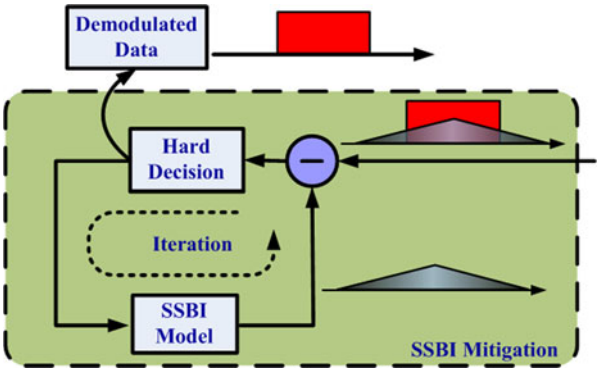

Fig. 5. Schematic diagram of iterative SSBI mitigation.

Using Eq. (3), SSBI can be deterministically rebuilt with full knowledge of the transmitted data. However, the transmitted data cannot be precisely determined at the receiver. Thus, hard decisions are required to obtain quantized data $\hat{D}_{i,n}$, from $\tilde{D}_{i,n}$, such that $\hat{D}_{i,n}$ is used to emulate the correct transmitted data and calculate the SSBI via Eq. (3). As shown in Fig. 5, the reconstructed SSBI is then used to subtract the actual SSBI from the SSBI-interfered data. Decision errors can lead to inaccuracies in SSBI reconstruction and incomplete SSBI mitigation; however, this study adopted an iterative process to reduce the number of decision errors in the SSBI mitigation algorithm.

It should be noted that the bandwidth of SSBI (53.5–67.5 GHz) exceeds the 7-GHz allocated by the FCC, and no specific filter is available to eliminate a sufficient amount of out-of-band frequency components. Fortunately, the proposed SSBI mitigation process does not require information related to out-of-band frequency components, and the OFDM signal is unaffected by out-of-band frequency components. Furthermore, in the RAUs and receiver antenna units, 3-dB bandwidth of low noise amplifiers (LNA)s and filters are all 10 GHz (55–65 GHz), such that 4-GHz bandwidth of SSBI has been filtered out. Therefore, the influence of out-of-band frequency components is not very of notable concern.

III. Experimental Setup

Fig. 6 presents a schematic depiction of the experimental setup used in the proposed V-band RoF system using a 2 × 2 MIMO scheme. To realize the full 7-GHz of unlicensed bandwidth with a central frequency of 60.5 GHz, we encoded OFDM signals with a width of 3.5-GHz using Matlab which were implemented using a Tektronix® AWG7122B arbitrary waveform generator (AWG). The baseband IQ signals were then up-converted to 30.25 GHz using an IQ-mixer with 30.25-GHz sinusoidal waves and local oscillator (LO) to obtain an OFDM signal with bandwidth of 7-GHz. The modulation format of the OFDM signal was 8-QAM, and the length of the inverse fast Fourier transform was 512. We adopted an OFDM signal comprising 298 subcarriers, with a CP length of 16. The resolution and sampling rate of the digital-to-analog converter were set at 8 bits and 12 GSample/s, respectively. An additional sinusoidal wave of 30.25-GHz was also combined as an electrical

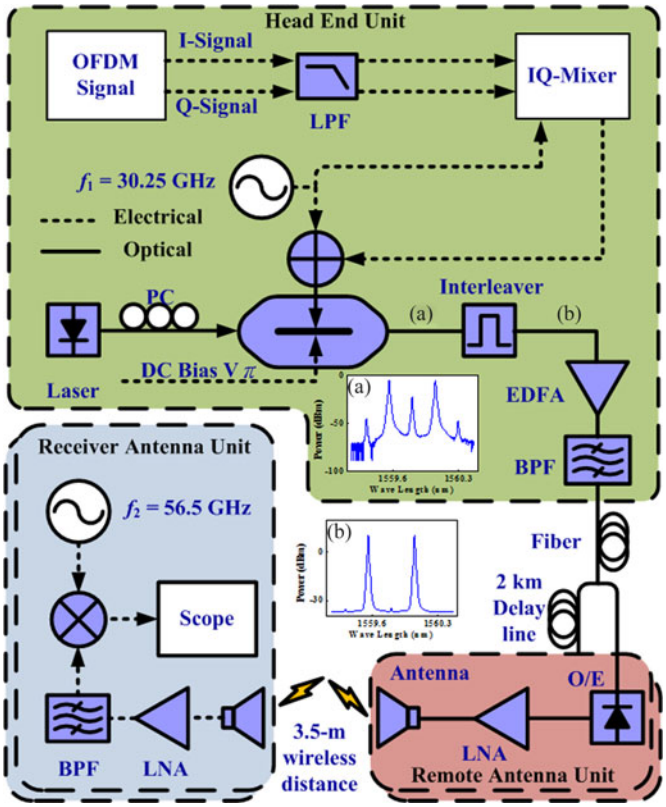

Fig. 6. Experimental Setup for the proposed 2 × 2 MIMO-OFDM RoF system.

carrier. After the coupler, the combined signal was used to drive a SD-MZM, biased at V_π to suppress the optical carrier signal. The source of the optical carrier signal was a DFB laser with a wavelength of 1558.9 nm and optical power of 16 dBm. Consequently, each sideband comprised an OFDM-modulated signal and a single tone with a central frequency of $f_c \pm 30.25$ GHz. An optical interleaver (33/33 GHz) was inserted after the SD-MZM to further suppress the laser carrier. The optical spectra are presented in the insets of Fig. 6. An Erbium-doped fiber amplifier with 4.3-dB noise figure was used to provide optical power gain followed by an optical band-pass filter with 3-dB bandwidth of 0.9 nm to suppress the amplified spontaneous emission noise. Following transmission of 0 to 14-km along a standard single mode fiber, the optical signal was split into two duplicates before reaching the RAU in order to emulate the two RoF signals required for the proposed 2 × 2 MIMO system. The independent formation of the two optical signals involved an additional standard single mode fiber, 2-km in length, combined with a dispersion-compensation fiber as a dispersion-free delay line for the de-correlation of the two duplicate signals. In this manner, two entirely de-correlated data signals were sent into the two 67-GHz photo-detectors, after which, the beating terms of the optical signals comprised two 60.5-GHz OFDM signals as well as two SSBI. Each 60.5-GHz signal was then amplified using a LNA, and launched into a 3.5-m MIMO wireless channel using a rectangular waveguide-based standard gain horn antenna. Following air transmission, the 60-GHz wireless signals were received by another pair of standard gain horn antennas and

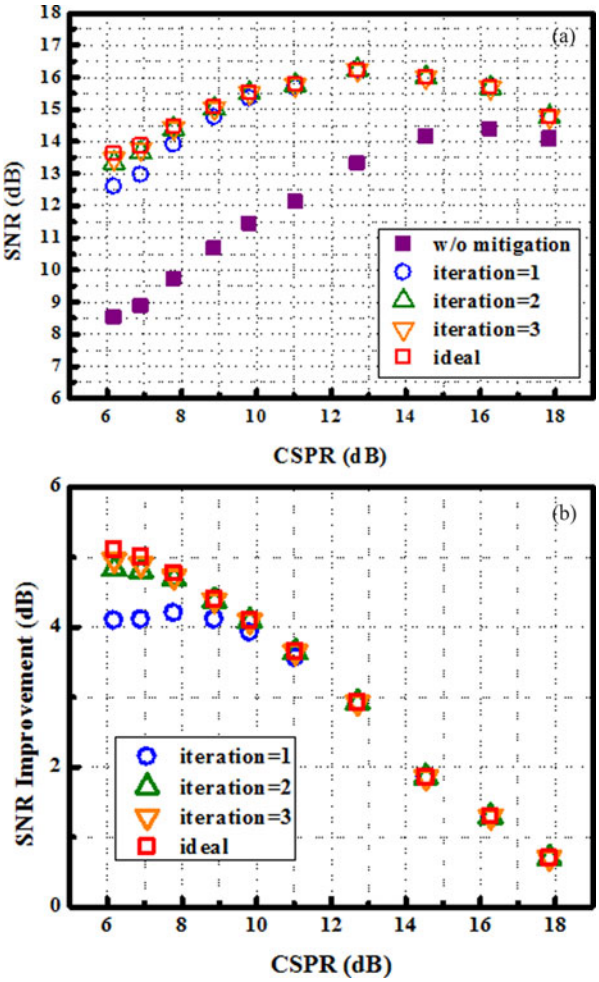

Fig. 7. (a) The average SNRs of two received 60-GHz 8-QAM OFDM signals versus different CSPR. (b) The average SNR improvements of two received 60-GHz 8-QAM OFDM signals versus different CSPR.

again amplified using LNAs. After passing a band-pass filter (55∼65 GHz), each received signal was down-converted to an intermediate frequency of 5 GHz using a 56.5-GHz sinusoidal wave generated by the 28.25-GHz LO and a frequency doubler. An Agilent® DSA-X 91604A real-time oscilloscope with 80-GSample/s sampling rate and 3-dB bandwidth at 16 GHz was used to capture the down-converted signals, whereupon the captured signals were demodulated using offline digital signal processing including MIMO demodulation and SSBI mitigation. The bit-error-rate of the OFDM signals was measured by error counting.

IV. Experimental Result and Discussion

The carrier-to-signal power ratio (CSPR) is a crucial parameter in optimizing the performance of the proposed system. In this work, the CSPR of the generated OFDM signals was measured after being captured by the oscilloscope. Fig. 7(a) presents the relationship between CSPR and the measured signal-to-noise ratio (SNR). Without SSBI mitigation, the optimal CSPR was 16.3 dB. When CSPR was below the optimal value, performance was dominated by SSBI and when CSPR exceeded the optimal value, performance was dominated by noise. Mitigating SSBI enabled a reduction in the influence of SSBI, resulting in a decrease in the optimal CSPR to 12.7 dB. When the CSPR exceeded the optimal value, the major impairment was not SSBI but noise introduced into the RoF system. As shown in Fig. 7(b), high CSPR enabled the subtraction of SSBI from the desired signal using only one iteration of the mitigation algorithm in order to attain optimal performance. Conversely, when CSPR was low, SSBI dominated system performance, which required a greater number of iterations for the estimation of SSBI. To examine the upper limits of the SSBI mitigation algorithm, we employed SSBI mitigation under ideal conditions implemented with the full knowledge of the original transmitted data rather than using the hard decisions of the equalized received signal. With a sufficient number of iterations, the proposed iterative SSBI mitigation proved capable of performing as well as ideal SSBI mitigation.

Fig. 8(a) presents the BER curves of 2×2 MIMO 8-QAM OFDM signals with an optimal CSPR of 12.7 dB. Using the proposed iterative SSBI mitigation algorithm, the BER of the signal with -1-dBm received power was still able to meet the forward-error-correction limit (3.8×10^{-3}) over 12-km fiber transmission. Fig. 8(b) presents the constellations after a fiber transmission distance of 0 (back-to-back, BTB), 6, and 12 km with/without the proposed iterative SSBI mitigation. Using the same optimal CSPR of 12.7 dB, we were able to accurately estimate and entirely eliminate SSBI in the case of BTB. However, with an increase in the distance of fiber transmission, dispersion-induced RF power fading resulted in the deterioration of system performance. Moreover, due to the iterative nature of the SSBI mitigation algorithm, hard decision errors tended to propagate in the iteration loop, resulting in error propagation, which ultimately reduced the accuracy of estimating SSBI, even after fiber transmission of only a few kilometers.

To illustrate the effects of RF power fading and hard decision errors, Fig. 9 presents the SNR of each OFDM subcarrier with and without the proposed iterative SSBI mitigation algorithm. With the aid of SSBI mitigation, a conspicuous improvement in SNR was obtained in transmission distances within 8-km fiber. Moreover, the subcarriers in the central band suffer from SNR penalties caused by error propagation in the SSBI mitigation algorithm at transmission distances of 12-km fiber.

Fig. 10 presents the average SNR of two received signals, which decreased with an increase in fiber transmission distance. The SNR in the blue line was measured after the MIMO detector, and the SNR in the red line was measured following the MIMO detector and SSMI mitigation. Under the conditions of BTB and 12-km transmission, the proposed iterative SSBI mitigation algorithm provided an improvement in SNR of approximately 2.4- and 1.8-dB, respectively.

Fig. 11 presents the data rates attainable at various fiber transmission distances. To maximize the data rate, we applied the Levin-Campello bit-loading algorithm to optimize the OFDM signals over a channel with uneven frequency response [21] and dispersion-induced RF power fading. With a given target BER of 3.8×10^{-3} and fixed signal bandwidth of 7-GHz, the modulation order (i.e. number of bits) and the power of each

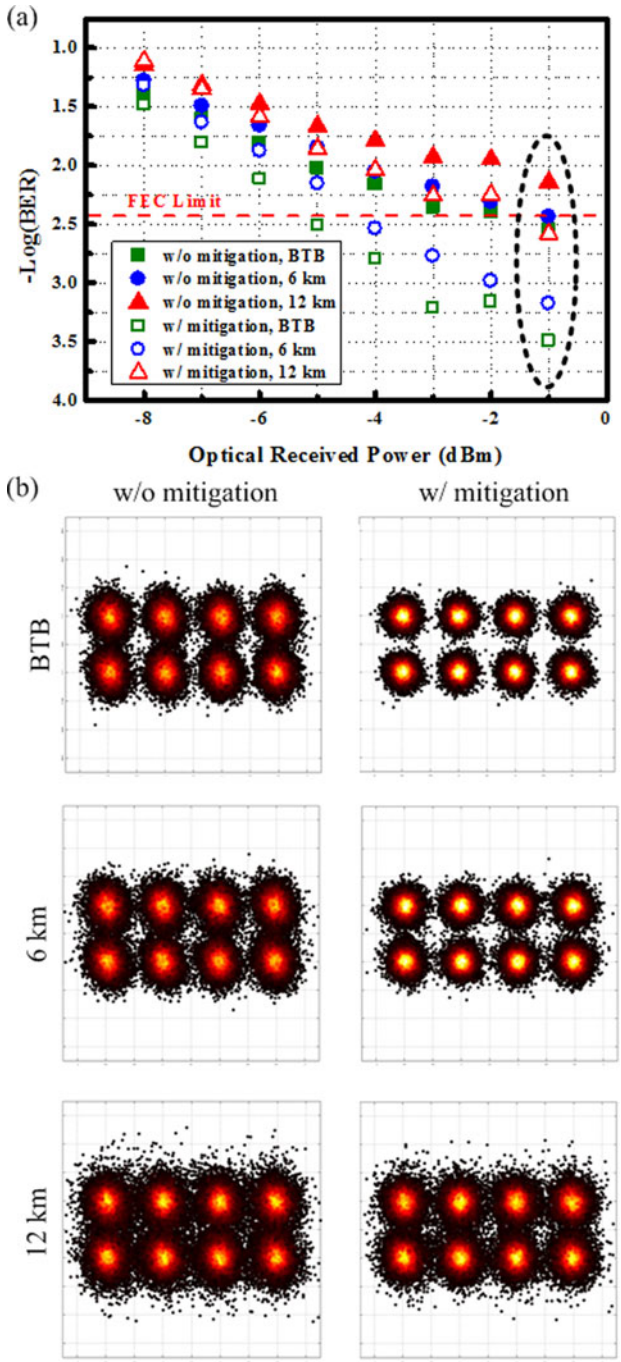

Fig. 8. (a) Average BER curves of two received 8-QAM OFDM signals versus different fiber transmission distance (3.5-m wireless distance included). (b) Received constellation corresponding to BTB, 6-km, 12-km fiber transmission.

subcarrier was adaptively allocated according to the measured SNR of the subcarriers. Data rates exceeding 50 and 40 Gb/s were attained after 8- and 12-km fiber transmission, respectively. Fig. 11 presents constellation diagrams with and without SSBI mitigation at 8 km, in which 16- and 8-QAM formats were adopted. Furthermore, in the case of optical BTB, the proposed iterative SSBI mitigation algorithm improved capacity by more than 10-Gb/s, resulting in a maximum data rate of 55.875-Gb/s using all subcarriers modulated in 16-QAM

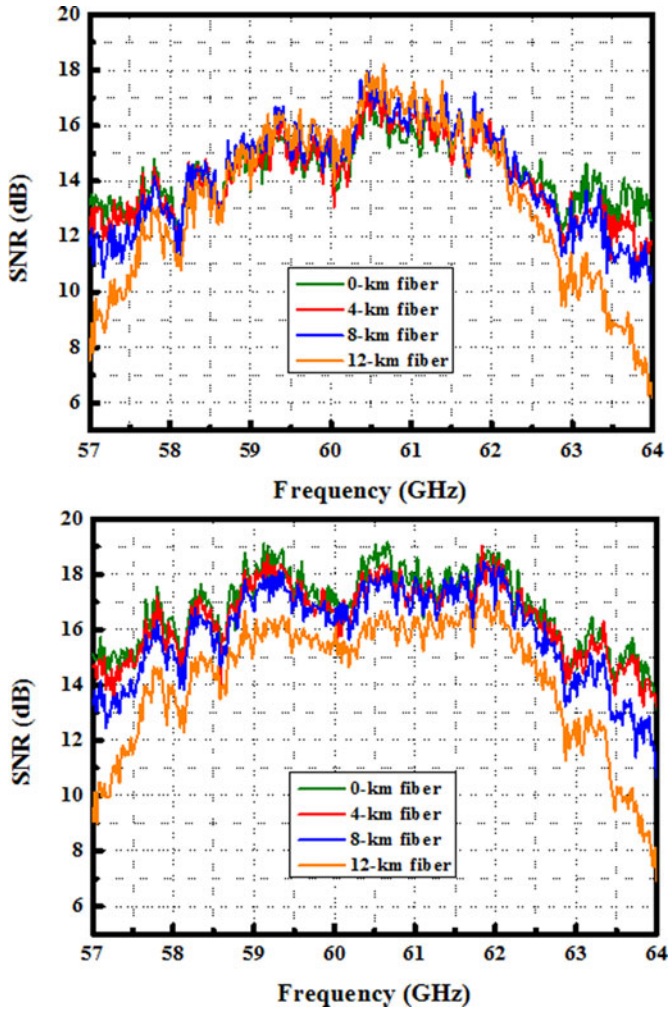

Fig. 9. SNR of each subcarrier within 7-GHz bandwidth centered at 60.5 GHz. (a) Without SSBI mitigation. (b) With SSBI mitigation.

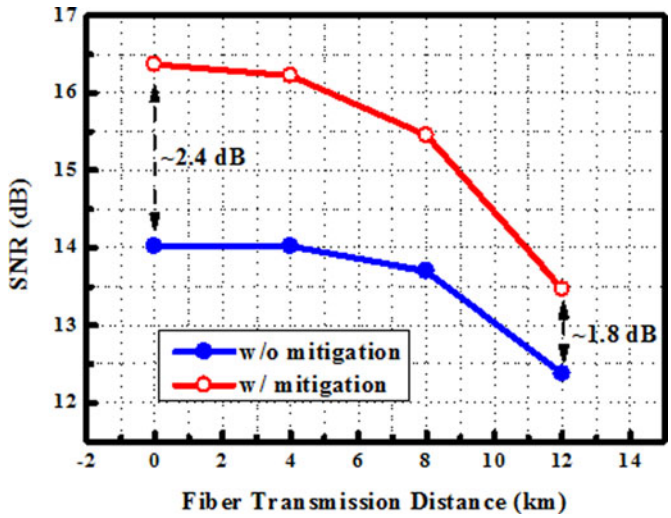

Fig. 10. Average SNR improvement versus different fiber transmission distance (3.5-m wireless distance included).

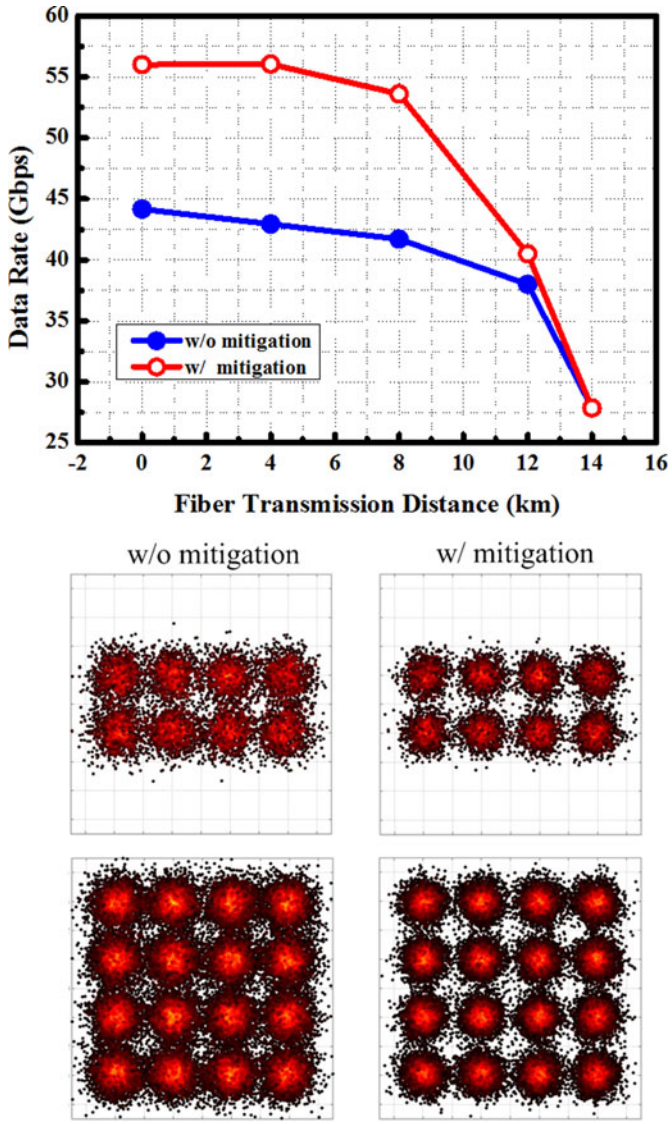

Fig. 11. Reachable data rate with adaptive bit-loading algorithm adopted.

format. With longer fiber transmission distances, the improvement in capacity provided by the proposed iterative SSBI mitigation algorithm was not as pronounced due to a decrease in SNR improvement. Eventually, at a transmission distance of 14 km, the capacity improvement was negligible, such that performance was dominated by dispersion-induced RF power fading.

V. Conclusion

This work demonstrated a 2 × 2 OFDM-modulated MIMO RoF communication system. Using the proposed frequency arrangement, RF power fading was limited to less than 10 dB over 12-km fiber transmission. In addition, with the aid of an iterative SSBI mitigation algorithm, the SSBI could be subtracted from both received signals to further increase system performance, resulting in an SNR improvement of 1.8 dB over 12-km fiber transmission. In addition, the use of the Levin-Campello rate-adaptive bit-loading algorithm in the 2 × 2 MIMO system improved the data rate to a maximum of 55.875 and 40.497 Gb/s for the case of optical BTB and 12-km fiber transmission, respectively.

References

[1] Federal Communication Commission, "Code of federal regulation, title 47 telecommunications, part 15," Federal Communication Commission, Tile 47, Part 15, Sec. 15.255, 2008.
[2] H. Lehpamer, "Millimeter-wave radios in backhaul networks," Communication Infrastructure Corporation, Tech. Paper, 2008.
[3] K. Kitayama, "Highly stabilized millimeter-wave generation by using fiber-optic frequency-tunable comb generator," *J. Lightw. Technol.*, vol. 15, no. 5, pp. 883–893, May 1997.
[4] G. H. Smith, D. Novak, and C. Lim, "A millimeter-wave full-duplex fiber-radio star-tree architecture incorporating WDM and SCM," *IEEE Photon. Technol. Lett.*, vol. 10, no. 11, pp. 1650–1652, Nov. 1998.
[5] T. Sakamoto, S. Shinada, T. Kawanishi, and M. Izutsu, "Mullimeter-wave-band amplitude-shifted-keyed radio-on-fiber signal generation with a reciprocating optical modulator," presented at the European Conf. Optical Communication, Stockholm, Sweden, 2004, Paper FE2.
[6] M. Weiss, M. Huchard, A. Stöhr, B. Charbonnier, S. Fedderwitz, and D. S. Jäger, "60-GHz photonic millimeter-wave link for short- to medium-range wireless transmission up to 12.5 Gb/s," *J. Lightw. Technol.*, vol. 26, no. 15, pp. 2424–2429, Aug. 1, 2008.
[7] A. Ng'oma, M. Sauer, F. Annunziata, W. J. Jiang, C. T. Lin, J. Chen, P. T. Shi, and S. Chi, "14 Gbps 60 GHz RoF link employing a simple system architecture and OFDM modulation," in *Proc. IEEE Int. Top. Meet. Microw. Photon.*, Valencia, Spain, Oct. 2009, pp. 1–4.
[8] J. Yu, Z. Jia, L. Li, Y. Su, G.-K. Chang, and T. Wang, "Optical millimeter wave generation or up-conversion using external modulator," *IEEE Photon. Technol. Lett.*, vol. 18, no. 1, pp. 265–267, Jan. 1, 2006.
[9] J. Yu, J. Gu, X. Liu, Z. Jia, and G.-K. Chang, "Seamless integration of an 8 × 2.5 Gb/s WDM-PON and radio-over-fiber using all-optical up-conversion based on raman-assisted FWM," *IEEE Photon. Technol. Lett.*, vol. 17, no. 9, pp. 1986–1988, Sep. 2005.
[10] A. Kanno, K. Inagaki, I. Morohashi, T. Sakamoto, T. Kuri, I. Hosako, T. Kawanishi, Y. Yoshida, and K. Kitayama, "40 Gb/s W-band (75–110 GHz) 16-QAM radio-over-fiber signal generation and its wireless transmission," *Opt. Exp.*, vol. 19, pp. B56–B63, Jul. 2011.
[11] T. Kuri, K. Kitayama, and Y. Ogawa, "Fiber-optic millimeter-wave uplink system incorporating remotely fed 60-GHz-band optical pilot tone," *IEEE Trans. Microw. Theory Techn.*, vol. 47, no. 7, pp. 1332–1337, Jul. 1999.
[12] W. J. Jiang, C. T. Lin, A. Ng'oma, P. T. Shih, J. Chen, M. Sauer, F. Annunziata, and S. Chi, "Simple 14-Gb/s short-range radio-over-fiber system employing a single-electrode MZM for 60-GHz wireless applications," *J. Lightw. Technol.*, vol. 28, no. 16, pp. 2238–2246, Aug. 15, 2010.
[13] C. T. Lin, J. Chen, P. T. Shih, W. J. Jiang, and S. Chi, "Ultra-high data-rate 60 GHz radio-over-fiber systems employing optical frequency multiplication and OFDM formats," *J. Lightw. Technol.*, vol. 28, no. 16, pp. 2296–2306, Aug. 15, 2010.
[14] W. Chen, T. H. Lu, C. Lin, C. Wang, C. Wei, C. Ho, F. Wu, and Y. Zhang, "Transmission distance improvement employing simple 60 GHz radio-over-fiber system with beat noise mitigation," presented at the Opt. Fiber Commun. Conf., 2012, Paper OM2B.4.
[15] X. Li, Z. Dong, J. Yu, N. Chi, Y. Shao, and G. K. Chang, "Fiber wireless transmission system of 108-Gb/s data over 80-km fiber and 2 × 2 MIMO wireless links at 100GHz W-Band frequency," *Opt. Lett.*, vol. 37, no. 24, pp. 5106–5108, 2012.
[16] L. Tao, Z. Dong, J. Yu, N. Chi, J. Zhang, X. Li, Y. Shao, and G. K. Chang, "Experimental demonstration of 48-Gb/s PDM-QPSK radio-over-fiber system over 40-GHz mm-wave MIMO wireless transmission," *IEEE Photon. Technol. Lett.*, vol. 24, no. 24, pp. 2276–2279, 2012.
[17] A. Kanno, T. Kuri, I. Hosako, T. Kawanishi, Y. Yasumura, Y. Yoshida, and K. Kitayama, "Optical and radio seamless MIMO transmission with 20-Gbaud QPSK," presented at the European Conf. Exhib. Opt. Commun., 2012, p. We.3.B.2.
[18] C. Lin, A. Ng'oma, W. Lee, C. C. Wei, C. Y. Wang, T. H. Lu, J. Chen, W. J. Jiang, and C. H. Ho, "2 × 2 MIMO radio-over-fiber system at 60 GHz employing frequency domain equalization," *Opt. Exp.*, vol. 20, no. 1, pp. 562–567, 2012.
[19] Q. H. Spencer, A. L. Swindlehurst, and M. Haardt, "Zero-forcing methods for downlink spatial multiplexing in multiuser MIMO channels," *IEEE Trans. Signal Process.*, vol. 52, no. 2, pp. 461–471, Feb. 2004.

[20] W. R. Peng, X. Wu, V. R. Arbab, K. M. Feng, B. Shamee, L. C. Christen, J. Y. Yang, A. E. Willner, and S. Chi, "Theoretical and experimental investigations of direct-detected RF-tone assisted optical OFDM systems," *J. Lightw. Technol.*, vol. 27, no. 10, pp. 1332–1339, May 2009.
[21] T.-N. Duong, N. Genay, M. Ouzzif, J. Le Masson, B. Charbonnier, P. Chanclou, and J. C. Simon, "Adaptive loading algorithm implemented in AMOOFDM for NG-PON system integrating cost-effective and low-bandwidth optical devices," *IEEE Photon. Technol. Lett.*, vol. 21, no. 12, pp. 790–792, Jun. 15, 2009.

Hou-Tzu Huang received the B.S. degree in the Department of Photonics from National Chiao Tung University, Hsinchu, Taiwan, in 2012. He is currently working toward the Ph.D. degree in the Institute of Photonics System, National Chiao Tung University, Tainan, Taiwan. His current research interests include radio-over-fiber systems, fiber/wireless multi-input multi-output technique and digital signal processing.

Chun-Ting Lin received the B.S. and M.S. degrees in material science and engineering from National Tsing Huang University, Hsinchu, Taiwan, in 1997 and 2001, respectively, and the Ph.D. degree in electro-optical engineering from National Chiao-Tung University, Hsinchu, in 2007. From 2007 to 2009, he was a Research Associate with the Department of Photonics, National Chiao Tung University, Hsinchu. In 2009, he joined as the faculty of National Chiao Tung University, where he is currently an Associate Professor with the Institute of Photonic System, National Chiao Tung University, Tainan, Taiwan. His current research interests include radio-over-fiber systems, optical millimeter/sub-terahertz wave generation and application, optical data formats, and opto-electronic packages.

Ya-Tang Chiang received the B.S. degree in physics from National University of Kaohsiung, Kaohsiung, Taiwan in 2011. He is currently working toward the M.S. degree in Department of Photonics, National Sun Yat-Sen University, Kaohsiung. His research interests include radio-over-fiber systems and digital signal processing.

Chia-Chien Wei received the Ph.D. degrees in electro-optical engineering from National Chiao Tung University, Taiwan, and in electrical engineering from the University of Maryland, Baltimore, MD, USA, in 2008. In 2011, he joined National Sun Yat-sen University, Taiwan, where he is currently an Assistant Professor at the Department of Photonics. His current research interests include optical and electrical signal processing, advanced modulation formats, optical access networks, and radio-over-fiber systems.

Chun-Hung Ho received the Bachelor degree from the Department of Electrical Engineering from National Taiwan Ocean University, Keelung, Taiwan, in 2009. He is currentlyworking toward the Ph.D. degree in the Institute of Photonic Systems at National Chiao Tung University, Tainan, Taiwan. His research interests include V/W-band Radio-over-Fiber system, digital13 signal processing, multi-input multi-output technique and millimeter wave generation. He is a student member of the Optical Society of America Society.